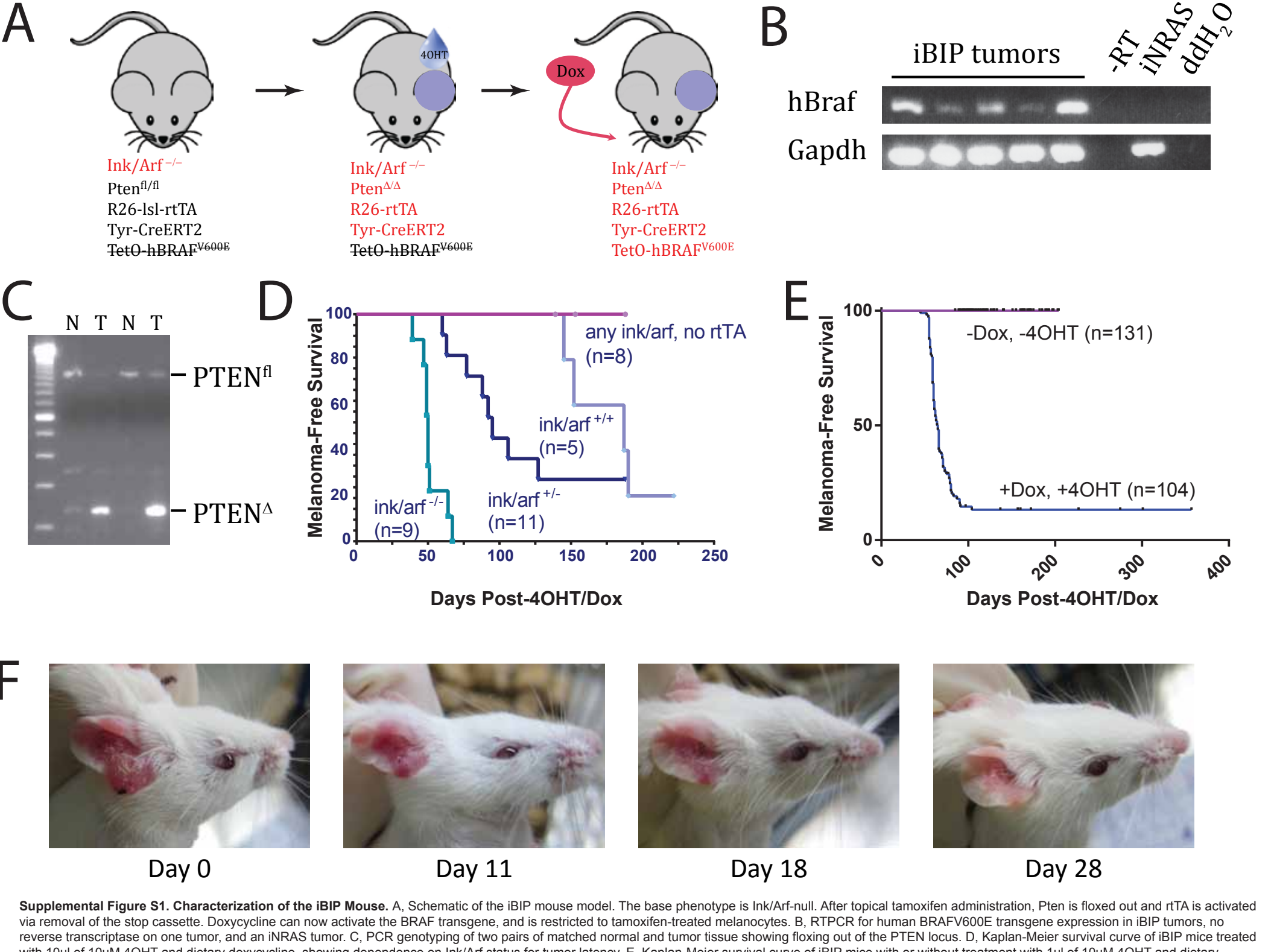

Supplemental Figure S1. Characterization of the iBIP Mouse. A, Schematic of the iBIP mouse model. The base phenotype is Ink/Arf-null. After topical tamoxifen administration, Pten is floxed out and rtTA is activated via removal of the stop cassette. Doxycycline can now activate the BRAF transgene, and is restricted to tamoxifen-treated melanocytes. B, RTPCR for human BRAFV600E transgene expression in iBIP tumors, no reverse transcriptase on one tumor, and an iNRAS tumor. C, PCR genotyping of two pairs of matched normal and tumor tissue showing floxing out of the PTEN locus. D, Kaplan-Meier survival curve of iBIP mice treated with 10ul of 10uM 4OHT and dietary doxycycline, showing dependence on Ink/Arf status for tumor latency. E, Kaplan-Meier survival curve of iBIP mice with or without treatment with 1ul of 10uM 4OHT and dietary doxycycline. F, representative mouse with longitudinal pictures showing tumor regression off doxycycline.

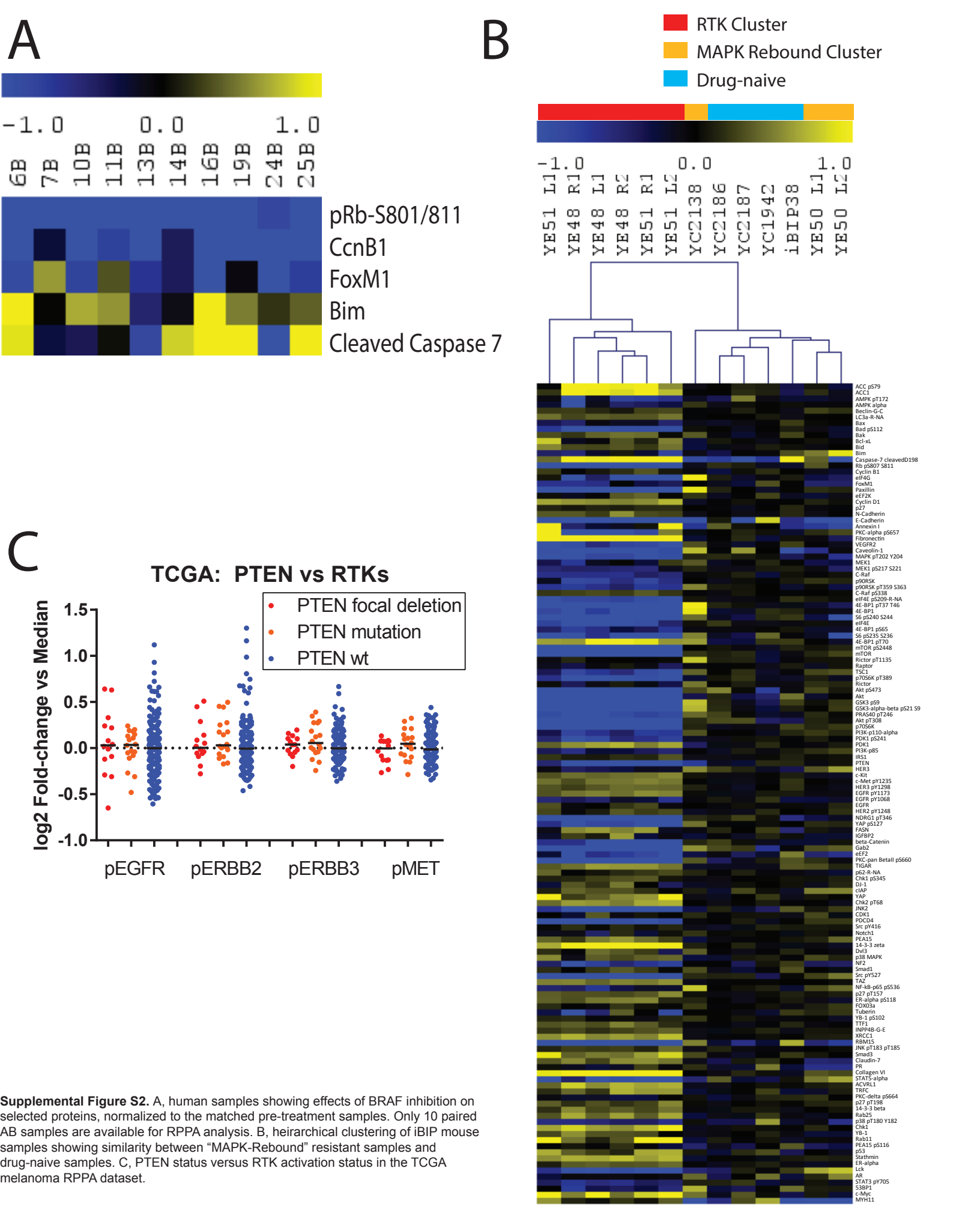

Supplemental Figure S2. A, human samples showing effects of BRAF inhibition on selected proteins, normalized to the matched pre-treatment samples. Only 10 paired AB samples are available for RPPA analysis. B, heirarchical clustering of iBIP mouse samples showing similarity between "MAPK-Rebound" resistant samples and drug-naive samples. C, PTEN status versus RTK activation status in the TCGA melanoma RPPA dataset.

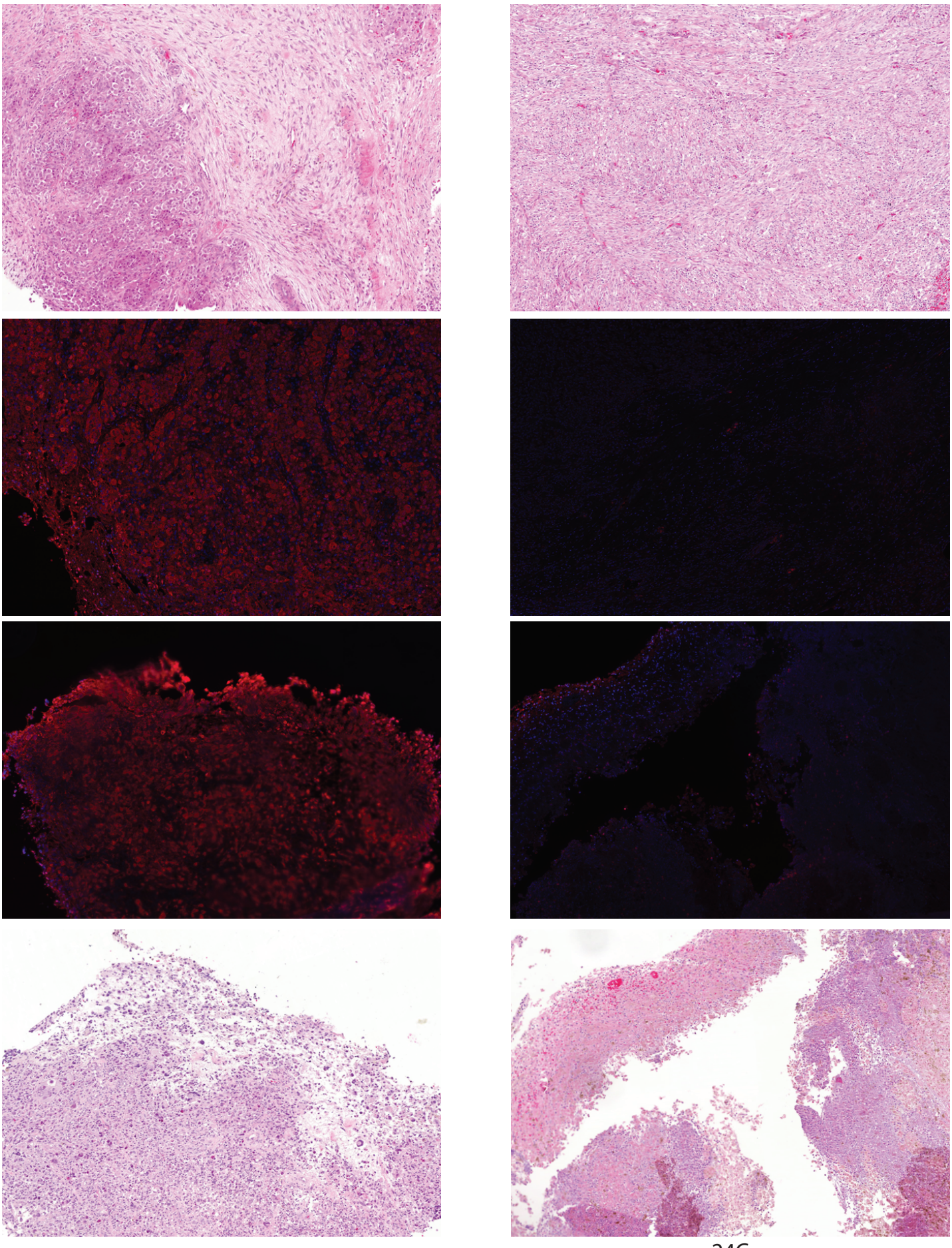

Supplemental Figure S3. Immunohistochemistry for pERK (red) and DAPI (blue) on human patient samples. H&E slides of the same area are also shown.

Supplemental Figure S4

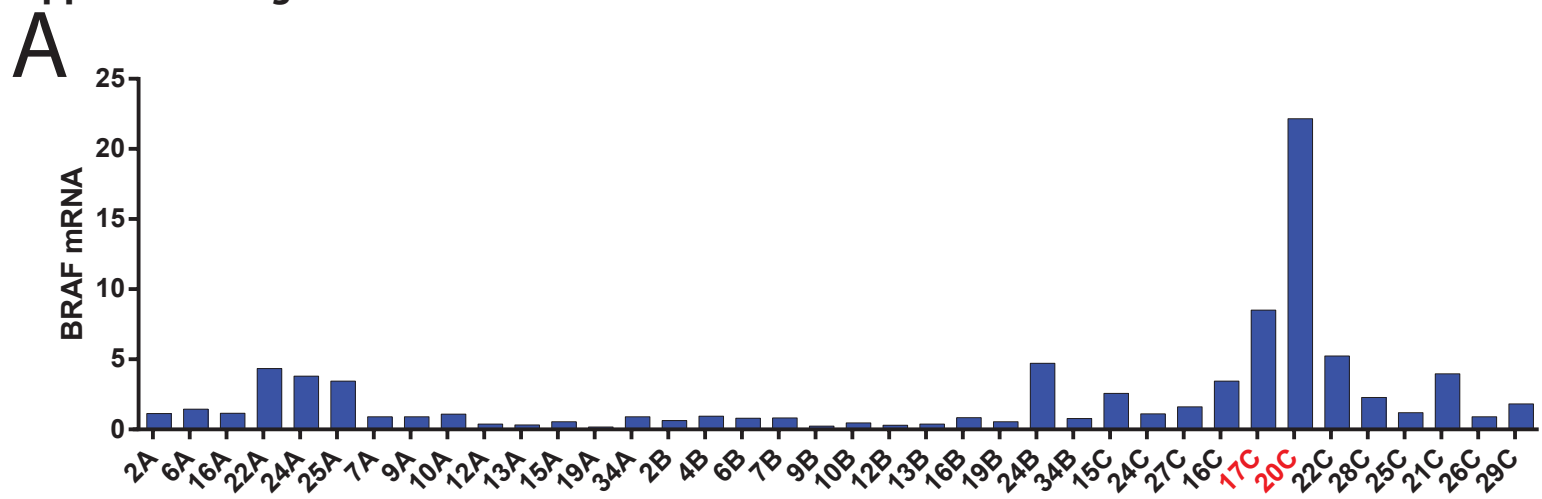

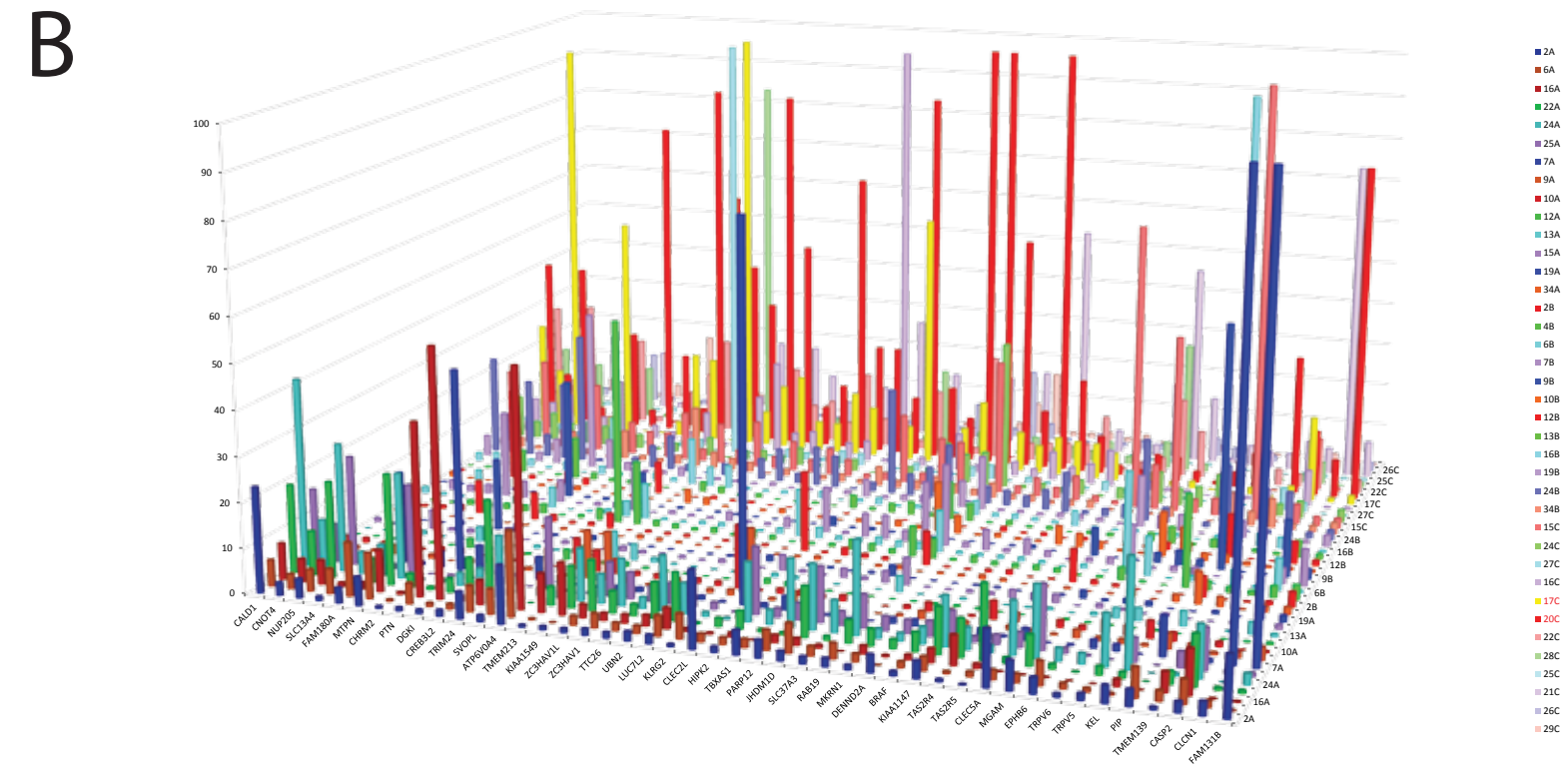

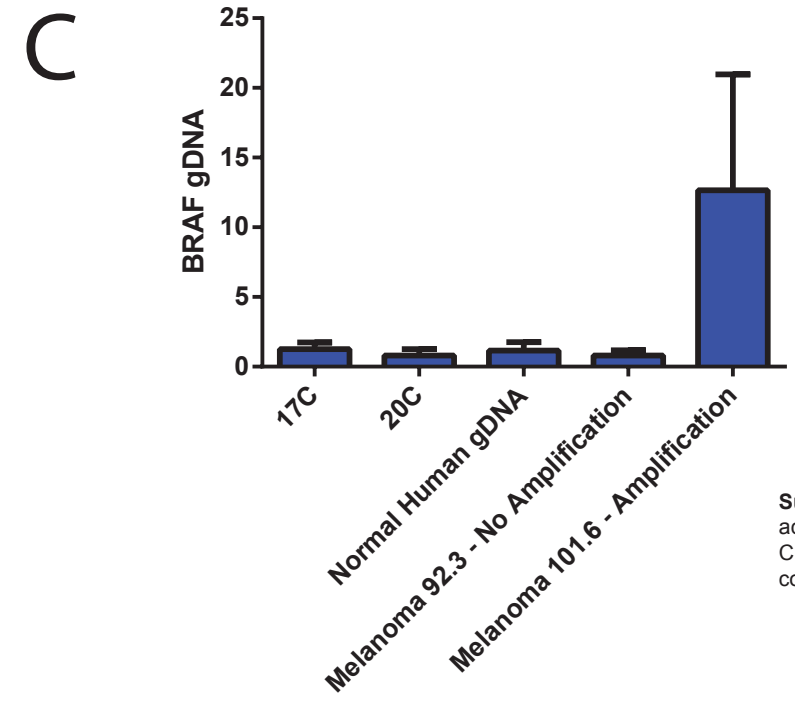

Supplemental Figure S4. Analysis of the BRAF locus. A, relative expression of BRAF across all human samples. B, relative expression of genes surrounding the BRAF locus. C, quantitative PCR analysis of the BRAF locus, including one negative and one positive control melanoma described in (47).

Supplemental Figure 5

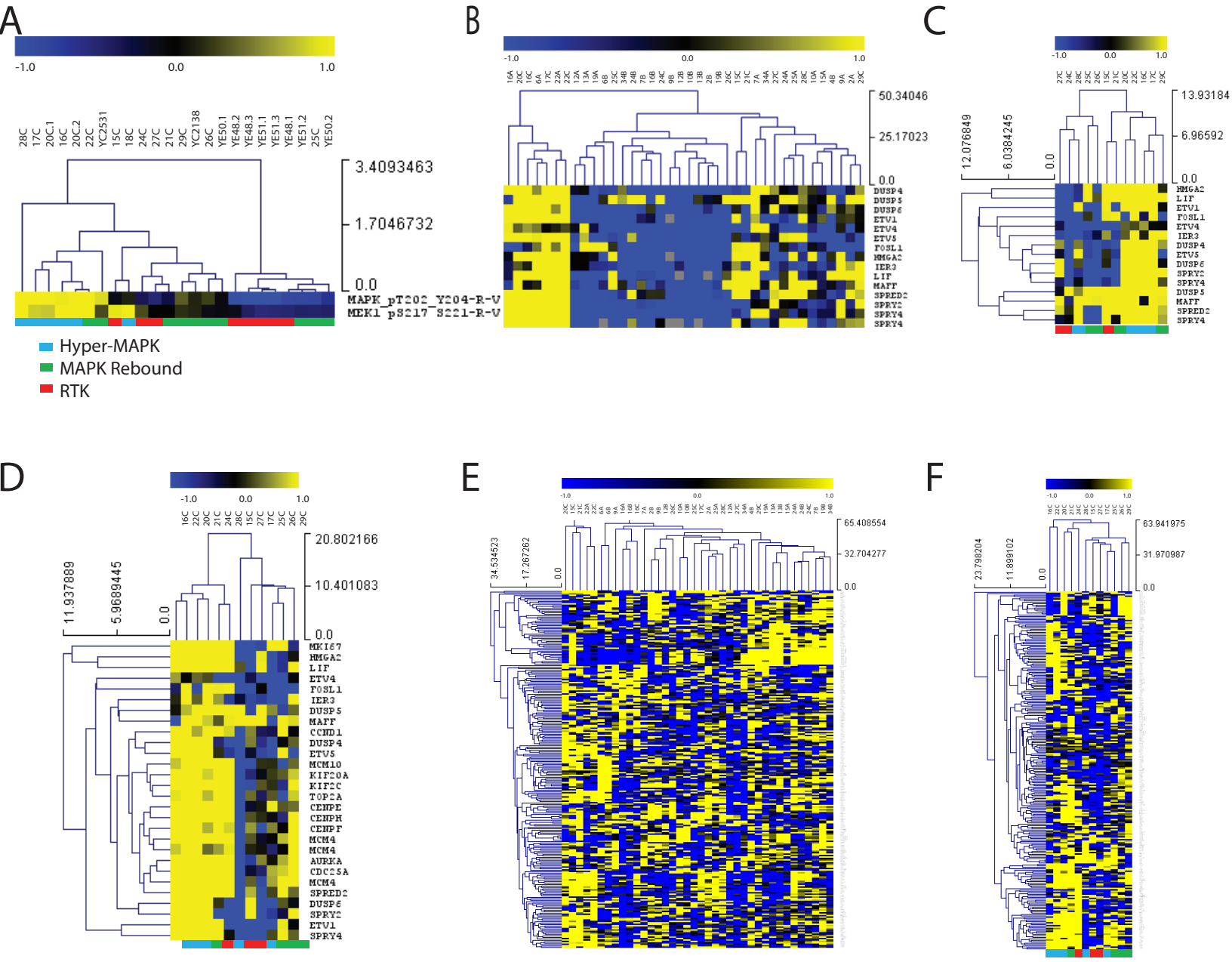

Supplemental Figure S5. Supervised and unsupervised clustering of RPPA and RNA-seq data. A, Clustering of resistant human and mouse samples solely by pERK and pMEK RPPA data. B,C Clustering by the RNA-seq ERK signature of B, all samples and C, all resistant samples. D, Clustering of all samples by the RNA-seq ERK and cell cycle signatures. E, F. Unsupervised clustering using the top 2.5% most variable genes for E, all samples and F, only the resistant

Supplemental Figure 6

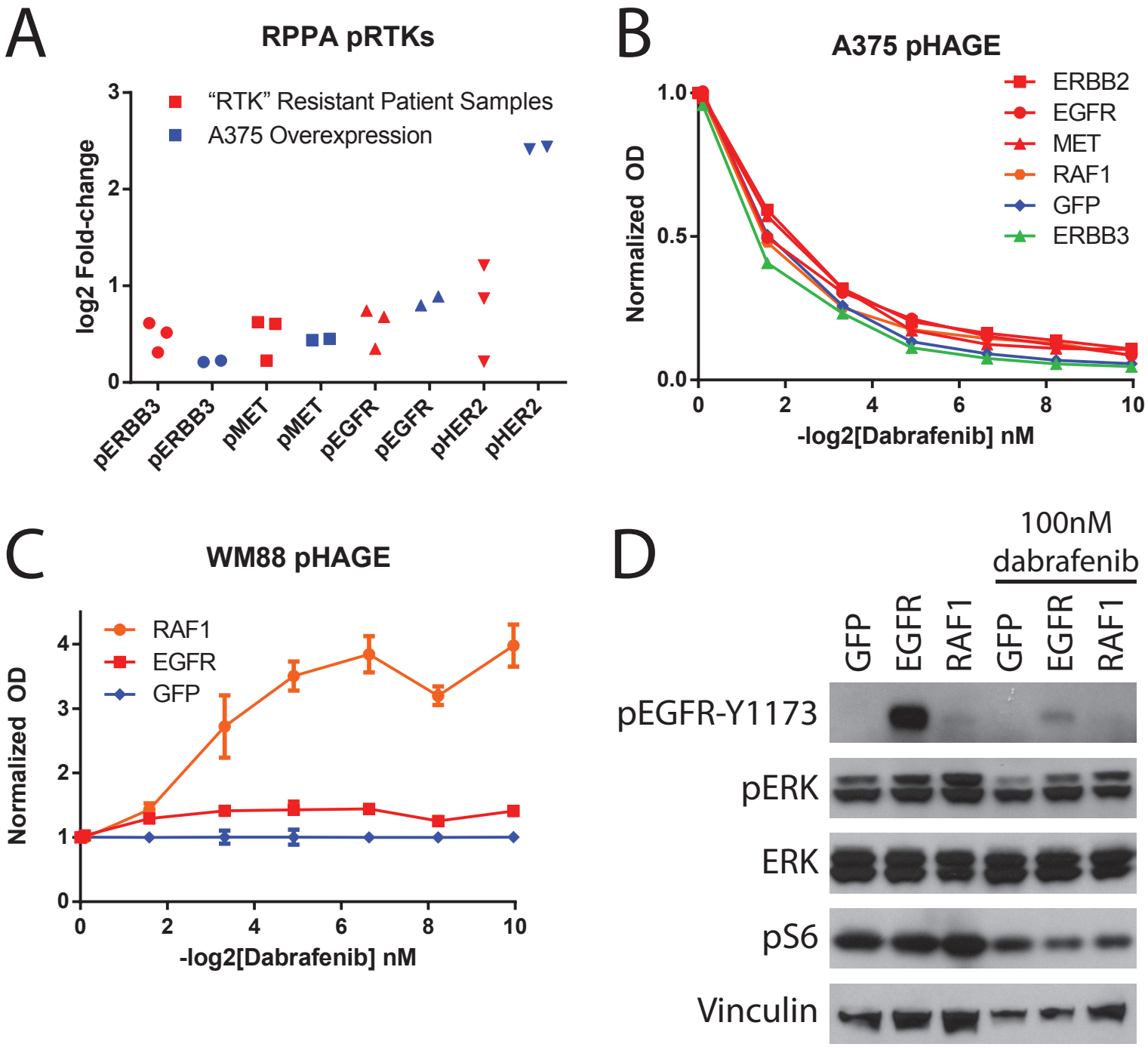

Supplemental Figure S6. In vitro RTK analyses. A, Quantification of RTK overexpression by RPPA, showing similar levels in A375 (vs GFP) and in patient "RTK" tumor samples (vs pretreatment samples). B, Unnormalized dose-response curve from Fig. 5A. C, effect of EGFR overexpression on WM88 growth in monolayer. D, Western blot of MAPK and mTOR pathway markers in the absence or presence of 100nM dabrafenib in WM88 cells.

Supplemental Figure S7

Pre-treatment vs PFS
Correlation
FWER = 0

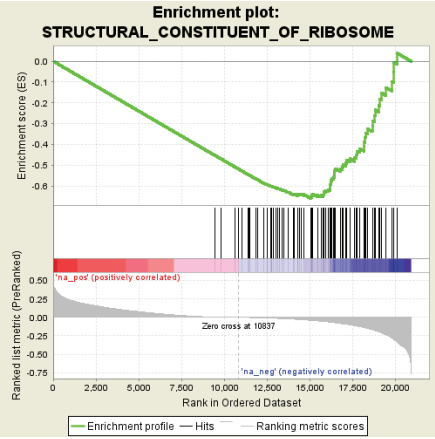

Pre-treatment vs PFS
Anti-Correlation
FWER = 0.009

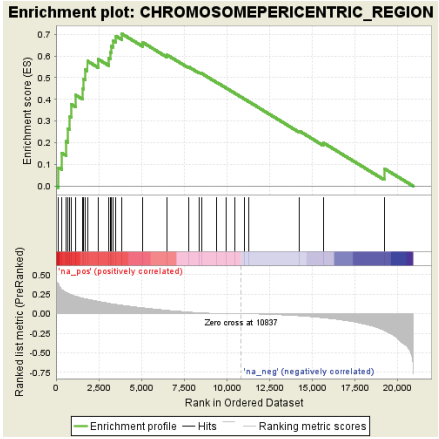

Pre-treatment vs RECIST
Correlation
FWER = 0.128

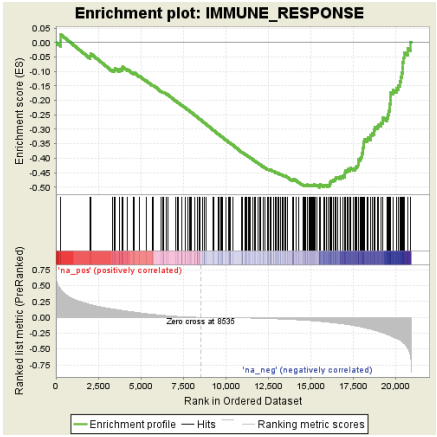

Pre-treatment vs RECIST
Anti-Correlation
FWER = 0.139

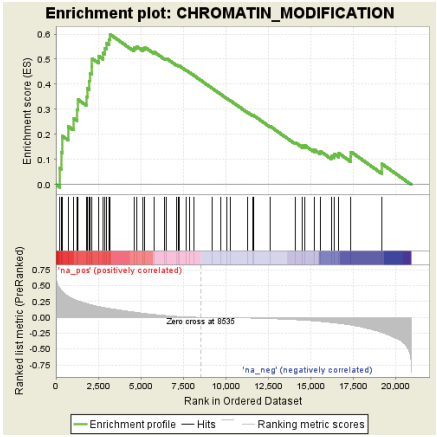

On-treatment vs PFS
Correlation
FWER = 0

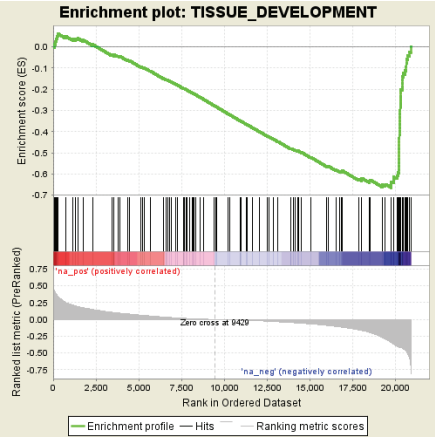

On-treatment vs PFS
Anti-Correlation
FWER = 0

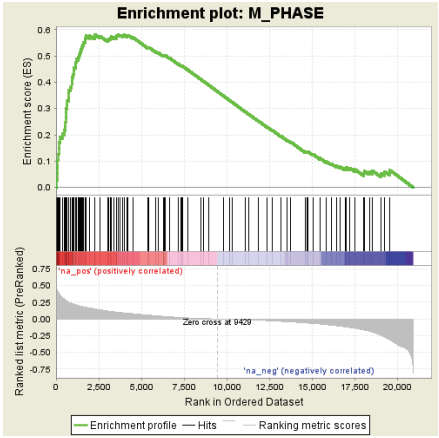

On-treatment vs RECIST
Correlation
FWER = 0

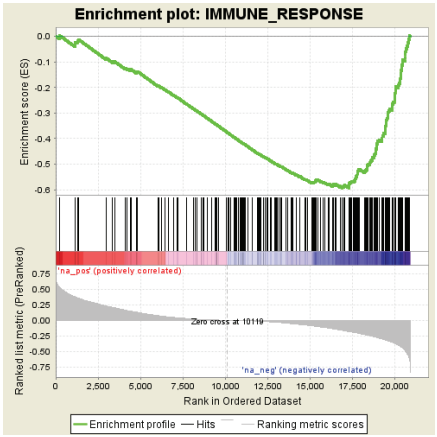

On-treatment vs RECIST
Anti-Correlation
FWER = 0.032

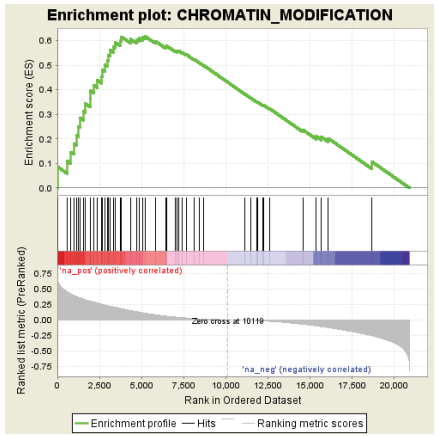

Supplemental Figure S7. GSEA plots of selected significant pathways identified for each sample-clinical outcome comparison.